Geomechanics and Engineering, *Vol. 15, No. 2 (2018) 775-781*
DOI: https://doi.org/10.12989/gae.2018.15.2.775

Seismic responses of a metro tunnel in a ground fissure site

Nina Liu[*1,2], Qiang-Bing Huang[**1,2], Wen Fan[1,2a], Yu-Jie Ma[3b] and Jian-Bing Peng[1,2c]

[1]*School of Geological Engineering and Geomatics, Chang'an University, Xi'an 710054, China*
[2]*Key Laboratory of Western China Mineral Resource and Geological Engineering, Ministry of Education, Xi'an 710054, China*
[3]*Xi'an China Highway Geotechnical Engineering Co., Ltd, Xi'an 710075, China*

(Received May 27, 2017, Revised September 13, 2017, Accepted December 5, 2017)

Abstract. Shake table tests were conducted on scaled tunnel model to investigate the mechanism and effect of seismic loadings on horseshoe scaled tunnel model in ground fissure site. Key technical details of the experimental test were set up, including similarity relations, boundary conditions, sensor layout, modelling methods were presented. Synthetic waves and El Centro waves were adopted as the input earthquake waves. Results measured from hanging wall and foot wall were compared and analyzed. It is found that the seismic loadings increased the subsidence of hanging wall and lead to the appearance and propagation of cracks. The values of acceleration, earth pressure and strain were greater in the hanging wall than those in the foot wall. The tunnel exhibited the greatest earth pressure on right and left arches, however, the earth pressure on the crown of arch is the second largest and the inverted arch has the least earth pressure in the same tunnel section. Therefore, the effect of the hanging wall on the seismic performance of metro tunnel in earth fissure ground should be considered in the seismic design.

Keywords: tunnel; ground fissure; model test; dynamic response

1. Introduction

It is well known that the dynamic response of the ground and underground structures during earthquake is quite different (Sun *et al.* 2011, Fattah *et al.* 2015 and Lee *et al.* 2017). Jesmani (2016) and Angin (2016) indicate that earthquakes can damage tunnels especially in geo-hazard sites such as the fault, the changing stratum and the ground fissure. The San-I No.1 tunnel was severely damaged in the Chi-Chi earthquake in 1999. The tunnel was 8 km away from the location of the surface rupture of the Chelungpu Fault. The tunnel was temporarily closed for repair and reinforced after the Chi-Chi earthquake (Cheng *et al.* 2012, Liu *et al.* 2016). Many instances of noticeable seismic tunnel damage were reported in 2008 Wenchuan earthquake. The Longxi tunnel and Zipingpu tunnel of the Duwen highway crossing two faults as F8 and F11 had serious damages as lining cracking, joint staggering and inverted arch uplifting. The survey after earthquakes also indicated damages of subway structures. The Chengdu subway project which is the nearest subway tunnel to the epicenter of Wenchuan earthquake had obvious damages in the shield tunnel as lining cracks, dislocation, leakage and so on. Majid (2016) carried out research for segmental tunnels when they are susceptible to faulting and found that tunnels have different mechanisms of failure at large exerted permanent ground displacement.

Xi'an is in the 8 degree seismic fortification intensity in the seismic intensity zoning of China, thus seismic design must be considered during construction. At the same time, 14 ground fissures have been identified in Xi'an city. The total extension length is more than 100 km, with the covering area about 150 km^2, almost the whole city. Monitoring data show that these fissures are still active, with the annual increase rate of about 2-16 mm/*y*. Previous investigations have shown that a series of damages in the ground and underground structures had been caused by the ground fissures (Peng *et al.* 2017).

The subway projects are usually designed along linear alignments, and therefore, it is difficult to completely avoid the earth fissure ground because fissures lay in the liner planning with the construction design. The Xi'an Metro Line I and Line II have been in operation. Both of them have several intersections with ground fissures. There are still some metro lines in design and construction; all of which have one or more intersections with the 14 ground fissures. In recent years, seismic activities have occurred frequently. It indicates that China is just undergoing the 5th seismic active period. Therefore, understanding the dynamic characteristics of subway tunnel becomes a key factor of the safety in urban lifeline engineering, especially when the seismic load and ground fissures load are coupled.

For the geo-hazard site, different methods have been carried out to analyze the geo-hazard as ground fissure and fault. The metro tunnel is influenced not only by the seismic activities but also by the movement of the ground fissures

∗Corresponding author, Associate Professor
E-mail: dcdgx16@chd.edu.cn
**Corresponding author, Professor
E-mail: dcdgx24@chd.edu.cn
[a]Professor
E-mail: fanwen@chd.edu.cn
[b]Engineer
E-mail: 2016126105@chd.edu.cn
[c]Professor
E-mail: dicexy_1@chd.edu.cn

ISSN: 2005-307X (Print), 2092-6219 (Online)

due to complex underground geological conditions; therefore, dynamic tests can provide insight to understand the segmented metro tunnel, soil stress and strain behaviors (Cambio *et al.* 2011, Kang *et al.* 2015, Yang and Li 2017). Peng *et al.* (2017) simulated the influence of ground fissure on stratum during earthquake by numerical method. The integrity of the site had been impacted by earthquake and the vibration characteristics had corresponding change. Chen *et al.* (2015, 2016) studied the acceleration response, the soil pressure and strain responses of shield tunnel in earthquake by numerical simulation and shaking table test. The model tests on the tunnel were focused on the tunnel dynamic response in geological environment of different soil layers and fault. He *et al.* (2014), Kim *et al.* (2017) published rigorous research results with detailed investigation of large section shield tunnel, underground water tunnel by shaking table test. He *et al.* (2014) also reported the safety length and damping layer of the tunnel based on the results of model test. However, the failure characteristics of ground fissures and faults movement have essential difference. Few research studies of the tunnels influenced by active ground fissures have been found in the literatures.

This study investigated the behaviors of a metro tunnel in the ground fissure site when subjected to seismic loadings by the shaking table model test. The dynamic responses of the tunnel and the ground fissure site were obtained. The effect of the acceleration, the earth pressure, strains of the tunnel, the uneven settling, original cracks and developing new cracks of the ground fissure site are examined. El Centro earthquake waves and synthetic Xi'an earthquake waves were used as the input earthquake loading. Based on the laboratory investigation, recommendations and design guidance will be provided as a scientific basis for subway engineering design and construction in ground fissure developed geological disaster areas.

2. Materials and methods

2.1 Geology characteristics

Xi'an ground fissure is originated the northwest side of Lintong-Chang'an fault in the Fenwei depressed Basin. The tectonics and excessive use of groundwater were the coupling reason for the original and development of ground fissures (Holzer *et al.* 1989, Burridge *et al.* 1989, Escandon *et al.* 1999, Rojas *et al.* 2002, Peng *et al.* 2017). The 14 ground fissures are numerically numbered f_1 to f_{14} from north to south, and all of them present the similar characteristics. In profile plane direction, all of the ground fissures are northeastern with southeastern tendency and angle tilt varies from 70^o to 85^o. Ground fissures have three-dimensional movement characteristics, for example, the vertical displacement of the hanging wall relatively to the foot wall, the horizontal extension, and the horizontal twisting. The vertical settling is the greatest, the horizontal extension is intermediate, and the horizontal twisting has the least impact. The ration of the three movements is 1:0.30:0.03. The influence of ground fissures to metro tunnels is controlled by vertical displacement (Peng *et al.* 2017).

Table 1 Specifications of the shaking table

Name	Parameter
Size	1.0 m×1.5 m
Max loading	2 000 kg
Shaking direction	Horizontal direction
Frequency	0.1~50 Hz

Table 2 Scale ratios of the tunnel model to prototype

Name	Similarity relationship	Scale ratio
Strain similarity ratio	$C_\varepsilon = \varepsilon_m / \varepsilon_p$	1
Geometry similarity ratio	$C_l = l_m / l_p$	1/40
Density similarity ratio	$C_\rho = \rho_m / \rho_p$	1
Elastic modulus similarity ratio	$C_E = E_m / E_p$	1/5
Displacement similarity ratio	$C_u = C_l$	1/40
Time similarity ratio	$C_t = C_l \sqrt{C_\rho / C_E}$	0.056
Frequency similarity ratio	$C_f = 1/C_t$	17.857
Stress similarity ratio	$C_\sigma = C_E \cdot C_\varepsilon$	1/5
Acceleration similarity ratio	$C_a = C_l / C_t^2$	8

Table 3 Material properties

Material	Cement	Flyash	Sand	Fine stone（3~5 mm）	Early strengthagent	Water
Mix proportion/%	1.0	0.257	2.209	3.177	0.02	0.457

Table 4 Physical-mechanical properties of the tunnel model

Name	Density (kN.m^{-3})	Concrete cube strength (MPa)	Elastic modulus (MPa)
Tunnel model	25.00	2.98	3.3×10^3

2.2 Shake table and similarity rule

The main specifications of the shaking table are listed in Table 1. The shake table was manufactured by MTS. Co. Ltd. USA. The lab of the Chang'an University reformed the system with the MTS Company for vibration and loading control. The input wave of the shake table could be the harmonic wave and the random seismic wave. It is hard for the dynamic model test to fully satisfy similarity rule because of the complexity of the simulation test (Altunisik 2017, Bayati and Soltani 2016). According to the existing experimental conditions and the main targets of the test, the similarity ratio of the length was found to be the basic parameter (Wang. *et al.* 2015). Material parameters of the tunnel prototype were adopted from Xi'an Metro II. The similarity ratios of the parameters are listed in Table 2, where physical variables with subscript *m* are used for the model, and physical variables with subscript *p* are used to describe the prototype.

According to the similarity ratios shown in Table 2, the soil of model test was chosen from the interaction site of ground fissures f_7 and the Xi'an Metro II. The ground fissure was simulated by fine sand. In the metro tunnel model, the steel bars of prototype are made of galvanized

steel wire mesh, and the property of concrete is listed in Table 3.

Material properties of the tunnel prototype were adopted from Xi'an Metro II. The material parameters which are used in model test are listed in Table 4.

Fig. 1 Shake table tunnel model setup

Fig. 2 Horseshoe shape tunnel model

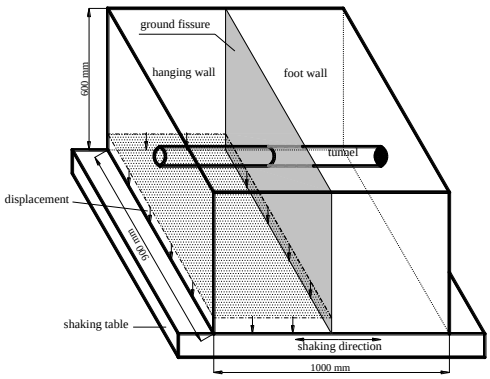

Fig. 3 Sketch of model casing

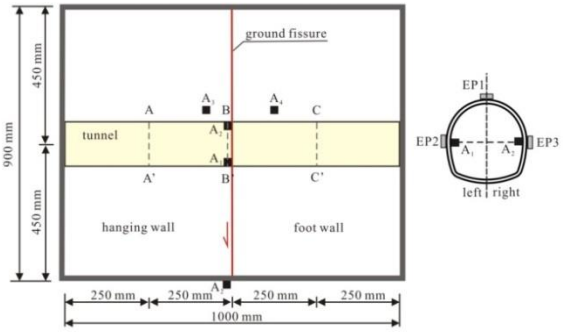

Fig. 4 Layout of monitoring points (unit: mm)

2.3 Boundary conditions of model casing

At present, three kinds of typical model casings are usually applied in the shaking table test, such as the rigid model casing, the laminar shear model casing and the cylindrical flexible model casing. In the design of the model casing, the boundary condition is expected to simulate the prototype foundation as much as possible. The boundary of the model casing may reproduce the seismic response of the free space in the vibration process, the boundary condition of the model casing is simple and clear, and convenient to collect the corresponding measurement data during the test. The shaking table test applied the rigid model casing based on the requirements (see Fig. 1). The model casing is made of the angle steel and the wood board. Some measures were adopted to assure synchronous vibration between the surrounding soil and the model casing, and to decrease the boundary effect. The polystyrene foam is 10 mm thick that was used to absorb seismic wave caused by reflection of box were pasted on the two inner sides of box. Wood screws were nailed each 100 mm at the bottom of the model casing to reduce the relative displacement and strengthen the friction between the soil and the bottom.

2.4 Test method

The model tunnel is based on a horseshoe shaped tunnel which is located in Xi'an Metro II intersected with ground fissure f_7. The model tunnel is shown in Fig. 2. From the design code as *specification for site investigation and engineering on Xi'an ground fractures* (DBJ 61-6-2006), the influence range of the ground fissure is 2.5 times of the tunnel external diameter in the hanging wall and 2.0 times of the tunnel external diameter in the foot wall. The length of prototype tunnel is 40 m, the external diameter is 4.5 m and the depth of the tunnel is 12 m. The tilt angle of ground fissure is 85^{o}, and the fissure is perpendicularly intersecting the tunnel. According to the prototype, the size of the model casing has 1.0 m length, 0.9 m width and 0.6 m height (see Fig. 3).

In order to analyze the dynamic response of the site and tunnel, the settling observation, resistance strain sensors, acceleration sensors and earth pressure cells are laid out and continuously sampled during the entire testing process (see Fig. 4). The data of the sensors are transported to computers which are installed outside the shaking table for recording. Further observations and measurements were conducted when the vibration stopped.

3. Results and discussions

3.1 Surface subsidence

The synthetic Xi'an earthquake wave and El Centro wave are loaded in the horizontal direction in order to observe the dynamic response and destruction of the tunnel model. The surface subsidence of the model site is shown in Fig. 5. On the surface of the model site, each 100 mm have a monitor point. The curves stand for the points lines from north to south, while the horizontal axis is east to west

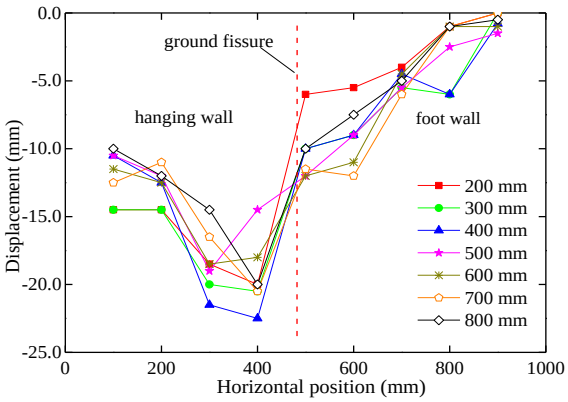

(a) Subsidence after El Centro wave

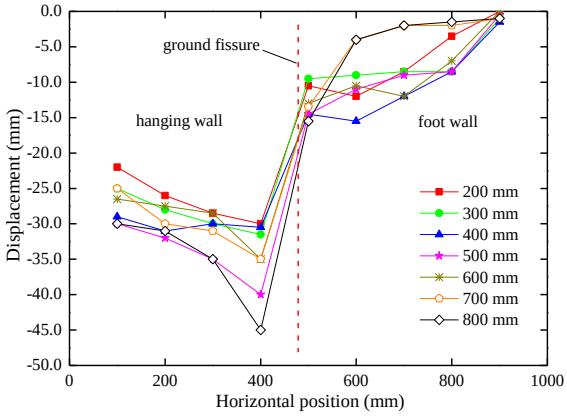

(b) Subsidence after synthetic Xi'an wave

Fig. 5 Measured surface subsidence

direction. From Fig. 5 it is clear that there is uneven settling in the ground fissure site. The rule of the displacement is very similar in the site no matter the input wave is El Centro or synthetic Xi'an earthquake wave. The greatest vertical displacement occurred in the hanging wall. The vertical displacement in the hanging wall is greater than that in the foot wall. The monitor points which are far away from the fissure in the foot wall almost didn't have settling. More close to the fissure, more vertical displacement in the hanging wall. The greatest displacements of each curve are located at the point of 400 mm in the horizontal axis which are the closest monitor points in the hanging wall. The greatest vertical displacement is 22.5 mm after the load of El Centro wave, and 45.0 mm after the synthetic Xi'an earthquake wave. Both of the vertical displacements are greater than the forecast value which is 2-16 mm/a. The earthquake load induced the vertical displacement of the ground fissure site, and increased more displacement than the forecast vertical displacement value.

3.2 Ground cracks

Cracks were appeared and expended with the loading of the earthquake wave. The first crack appeared on the surface of the hanging wall. More cracks were propagating and expending with the dynamic loading. A couple of cracks appeared on the foot wall. But the number of cracks in the foot wall is less than that in the hanging wall. The cracks are shown in Fig. 6. The Fig. 6(a) is a graphical

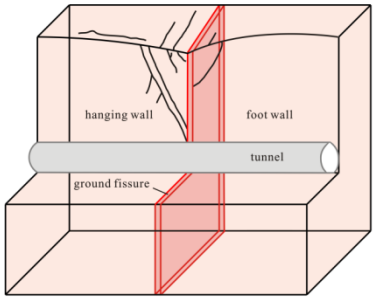

(a) Cracks in graphic model

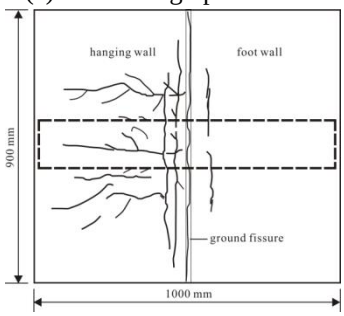

(b) Ground surface cracks

Fig. 6 The distribution of cracks after earthquake loading

model including the plan and the profile of the model site. It is shown that cracks caused by the earthquake appears at the hanging wall. Because the uneven settling of the site, the dynamic stress concentration appears in the location where close to the fissure when the vibration begins, and the stress concentration is more serious at the location where the fissure is the weak line in the vibration. With the increase of the vibration amplitude and the load duration of model casing, the surrounding soil reach the limit state of the crack, and then the first crack appears.

Cracks appeared on the hanging wall and foot wall, but the depth and the extending length of the cracks are different. The extending length of crack is longer, the depth and width are greater in the hanging wall than those of the cracks which are located in the foot wall. The biggest crack was observed in the shape "Y" combined with the fissure on the top of the tunnel in the hanging wall. The Fig. 6(b) is a plane graph of the surface cracks. The width of the widest crack is about 10 mm in hanging wall, and the width of the crack is about 2-3 mm in foot wall. As the result, the density and the width of the cracks in the hanging wall and the foot wall are different.

3.3 Model acceleration

Four acceleration sensors were located in the hanging wall, the foot wall and inside the tunnel which is shown in Fig. 4. The test acceleration peak value divisions the input peak is defined as magnification coefficient of acceleration (abbr. MC_a). The curve of MC_a and test point is shown in Fig. 7. The test acceleration can reliably express the dynamic characteristic of the tunnel, the hanging wall and the foot wall. From Fig. 7, an amplification effect on the ground fissure site and the metro tunnel is observed in the vibration process. The MC_a remains the same in the two test acceleration (A1 and A2) inside the tunnel which is 1.05.

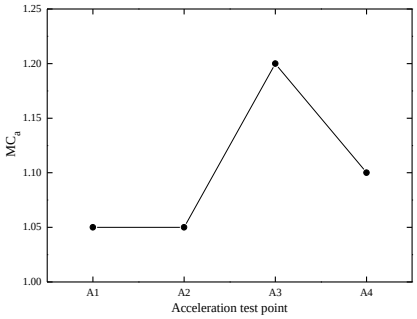

Fig. 7 Magnification coefficient of acceleration (MC_a)

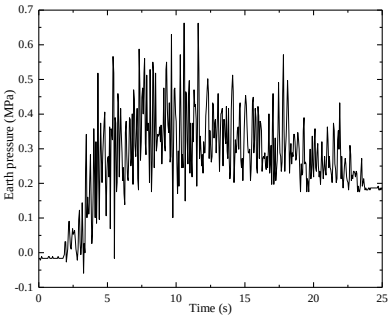

(a) EP1

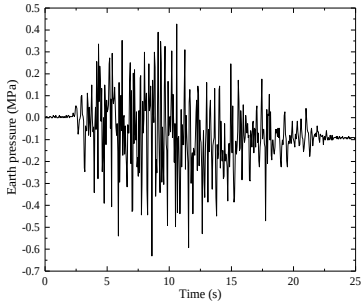

(b) EP2

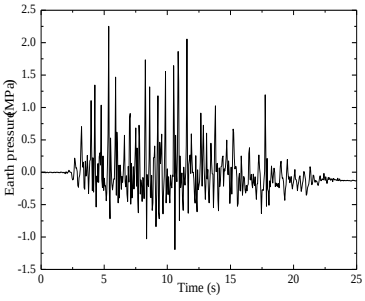

(c) EP3

Fig. 8 Time histories of earth pressure

The amplification effect of the tunnel is 5%. The tunnel has integrity character in the vibration process. The MC_a of A3 is 1.20 which is greater than that of A4 (1.10). The amplification effect of the hanging wall is 20%, and that is 10% of the foot wall; also both of them magnify the acceleration. No matter the hanging wall or the foot wall magnify the acceleration greater than that of the tunnel.

3.4 Earth pressure characteristics

In the test, micro earth pressure sensors were applied for monitoring the earth pressure of the model. The curves of earth pressure versus the time during the synthesis Xi'an earthquake loading are shown in Fig. 8. The earth pressure at every testing point is offset during the loading process and the offset cannot be eliminated after the vibration loading. In addition, the perpetual earth pressure at the top of the tunnel (EP1) is greater than that at the side wall (EP2 and EP3). The soil pressure of EP1 which located on the top of the tunnel is increased 0.2 MPa. The soil pressure of EP2 and EP3 decreased to 0.1 MPa and 0.15 MPa respectively.

The main reason the earth pressure offset is that the permanent deformation of the soil happened due to the earthquake loading which produced additional earth pressure in the tunnel structure. The restriction in the side wall of the tunnel by the surrounding soil is weaker so the earth pressure at the side wall is less. The earth pressure offset of EP1 which located at the top of the tunnel is 0.2 MPa and its permanent earth pressure is greater than that at any other location. The vibration of earthquake loading increased the earth pressure at the top of the tunnel.

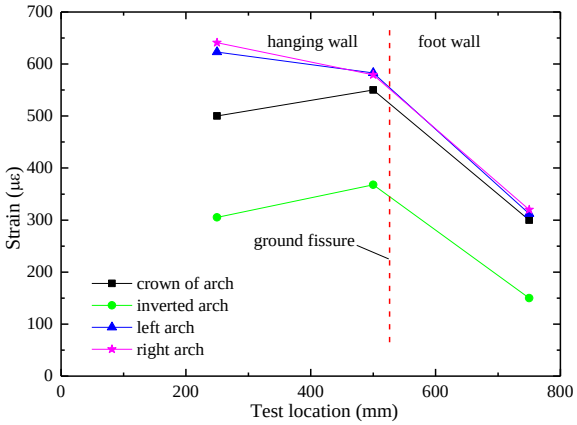

(a) El Centro wave

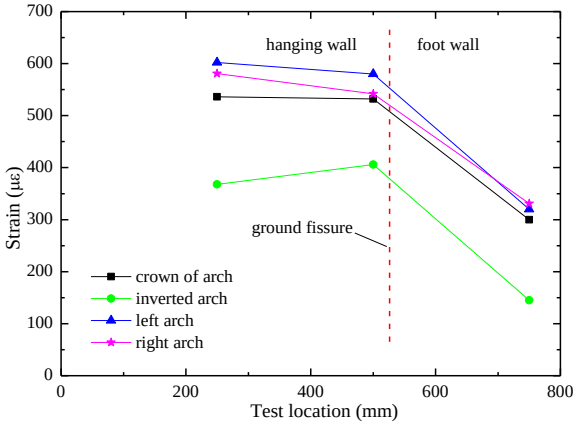

(b) The synthesis Xi'an earthquake wave

Fig. 9 Strain curves of tunnel in earthquake

3.5 Strain characteristics

In the test, the 5 mm×20 mm strain gauges were used for measuring the tunnel strain. The offset of the strains after synthesis Xi'an earthquake and El Centro earthquake are shown in Fig. 9. From Fig. 9 the strain characteristics after the vibration is known that the earthquake loading increased the strain at all locations. At the same cross-

section, the strains outside the left and right arch are the maximal strain. The strain on the crown of the arch is the second one while the strain of the inverted arch is the least one. Fig. 9(a) is the principal strains of tunnel after the loading of the El Centro earthquake wave. The strains of the left and right arch are a little more than 600 με in the hanging wall, while they are 300 με in the foot wall. The strain of the crown is 500 με in the hanging wall and it is about 300 με in the foot wall. The inverted arch has the strain less than the others part of the tunnel. The inverted arch only has the strain as 300 με in the hanging wall, and the strain is a little more than 100 με in the foot wall. Fig. 9(b) is the strains of the tunnel in the hanging wall and foot wall after the synthesis Xi'an earthquake wave. The curves of the strains have the same rule with the Fig. 9(a), and the strains have the similar value in the two kinds earthquake wave.

From the strains of the 3 testing cross-sections, the strains at the cross-section which located in the hanging wall are greater than those of the corresponding position in the foot wall. The tunnel in the hanging wall has greater deformation than that of the foot wall.

4. Conclusions

• Subsidence has been induced by the coupled earthquake and the ground fissure activities. The subsidence of hanging wall is greater than that in the foot wall, and it is greater than the predicted subsidence from the field survey. In the synthesis Xi'an earthquake, the deepest subsidence is about 45 mm in the range closing to the fissure.

• By the reason of the uneven settling between the hanging wall and the foot wall, the stress concentration, cracks appearing and propagating not only in hanging wall but also in the foot wall. More Cracks appeared in the hanging wall than that of the foot wall. And the extending length is longer, the depth and width are greater. The width is about 10 mm in the hanging wall and 2~3 mm in the foot wall.

• The amplification indicated by MC_a has the rule that the hanging wall has greater effect on amplification of dynamic loading than that of the foot wall. And the tunnel has the integrity character.

• The earth pressure at every testing point is offset in the dynamic duration. The earth pressure on the top of the tunnel is the greatest, the right and left arch have the similar values in the earth pressure.

• In the same cross-section, maximal strains were got outside the left and right arch. The strain on the crown of the arch is the intermediate one and that of the inverted arch is the smallest one. The perpetual strains at the cross-section which located in the hanging wall are greater than those of the corresponding positions in the foot wall.

Acknowledgements

The research has been supported by the National Natural Science Foundation of China (41502277, 41630634) and the Special Fund for Basic Scientific Research of Central Colleges, Chang'an University (300102268502). The authors acknowledge the support from the National Basic Research Program of China (973 Program) (2014CB744700).

References

Altunisik, A.C. (2017), "Shaking table test of wooden building models for structural identification", *Earthq. Struct.*, **12**(1)**,** 67-77.

Angin, Z. (2016), "Geotechnical field investigation on giresun hazelnut licenced warehause and spot exchange", *Geomech. Eng.*, **10**(4)**,** 547-563.

Bayati, Z. and Soltani, M., (2016), "Ground motion selection and scaling for seismic design of RC frames against collapse", *Earthq. Struct.*, **11**(3)**,** 445-459.

Burridge, P.B., Scott, R.F. and Hall, J.F. (1989), "Centrifuge study of faulting effects on tunnel", *J. Geotech. Eng.*, **115**(7), 949-967.

Chen, G.X., Chen, S., Zuo, X., Du, X.L., Qi, C.Z. and Wang, Z.H. (2015), "Shaking-table tests and numerical simulations on a subway structure in soft soil", *Soil Dyn. Earthq. Eng.*, **76**, 13-28..

Chen, Z., Chen, W. and Li, Y. (2016), "Shaking table test of a multi-story subway station under pulse-like ground motions", *Soil Dyn. Earthq. Eng.*, **82**,111-122.

Cheng, H.C., Tai, T.W. and Fu, S.J. (2012), "Mechanisms causing seismic damage of tunnels at different depths", *Tunn. Undergr. Sp. Technol.*, **28**, 31-40.

Escandon, R.F., Stirbys, A.F. and Radwanski, Z.R. (1999), "Los Angeles metro rail project-geologic and geotechnical design and construction constraints", *Eng. Geol.*, **51**(3), 203-224.

Fattah, M.Y., Hamoo, M.J. and Dawood, S.H. (2015), "Dynamic response of a lined tunnel with transmitting boundaries", *Earthq. Struct.*, **8**(1), 275-304.

He, C., Li, L. and Zhang, J. (2014), "Seismic damage mechanism of tunnels through fault zones", *Chin. J. Geotech. Eng.*, **36**(3), 427-434 (in Chinese).

Holzer, T.L. (1989), "State and local response to damaging land subsidence in US urban areas", *Eng. Geol.*, **27**(1-4), 449-466.

Jesmani, M., Kamalzare, M. and Sarbandi, B.B. (2016), "Seismic response of geosynthetic reinforced retaining walls", *Geomech. Eng.*, **10**(5)**,** 635-655.

Kang, X. and Kang, G.C. (2015), "Modified monotonic simple shear tests on silica sand", *Mar. Georesour. Geotechnol.*, **33**(2), 122-126.

Kim, Y.M., Kwon, T.H. and Kim, S. (2017), "Measuring elastic modulus of bacterial biofilms in a liquid phase using atomic force microscopy", *Geomech. Eng.*, **12**(5), 863-870.

Lee, J.Y., Jin, C.J. and Kim, M. (2017), "Dynamic response analysis of submerged floating tunnels by wave and seismic excitations", *Ocean Syst. Eng.*, 7(1), 1-19.

Liu, X.R., Li, D.L., Wang, J.B. and Wang, Z. (2015), "Surrounding rock pressure of shallow-buried bilateral bias tunnels under earthquake", *Geomech. Eng.*, **9**(4), 427-445.

Majid, K., Abbas, G. and Tohid, A. (2016), "Experimental evaluation of vulner ability for urban segmental tunnels subjected to normal surface faulting", *Soil Dyn. Earthq. Eng.*, **89**, 28-37.

Peng, J.B., Huang, Q.B. and Hu, Z.P. (2017), "A proposed solution to the ground fissure encountered in urban metro construction in Xi'an, China", *Tunn. Undergr. Sp. Technol.*, **61**, 12-25.

Rojas, E., Arzate, J. and Arroyo, M. (2002), "A method to predict the group fissuring and faulting caused by regional groundwater decline", *Eng. Geol.*, **65**(4), 245-260.

Sun, T.C., Yue, Z.R. and Gao, B. (2011), "Model test study on the dynamic response of the portal section of two parallel tunnels in a seismically active area", *Tunn. Undergr. Sp. Technol.*, **26**(2), 391-397.

Wang, Z.Z., Jiang, Y.J. and Zhu, C.A. (2015), "Shaking table tests of tunnel linings in progressive states of damage", *Tunn. Undergr. Sp. Technol.*, **50**, 109-117.

Yang, X.L. and Li, W.T. (2017), "Reliability analysis of shallow tunnel with surface settlement", *Geomech. Eng.*, **12**(2), 313-326.

JS